

Lucky Imaging survey for southern M dwarf binaries^{★,★★}

C. Bergfors^{1,★★★}, W. Brandner¹, M. Janson², S. Daemgen³, K. Geissler¹, T. Henning¹,
S. Hippler¹, F. Hormuth¹, V. Joergens^{1,4}, and R. Köhler^{1,5}

¹ Max-Planck-Institut für Astronomie, Königstuhl 17, 69117 Heidelberg, Germany
e-mail: bergfors@mpia.de

² University of Toronto, Dept. of Astronomy, 50 St George Street, Toronto, ON, M5S 3H8, Canada

³ European Southern Observatory, Karl-Schwarzschild Strasse 2, 85748 Garching, Germany

⁴ Zentrum für Astronomie Heidelberg, Institut für Theoretische Astrophysik, Albert-Ueberle-Str. 2, 69120 Heidelberg, Germany

⁵ Landessternwarte, Zentrum für Astronomie der Universität Heidelberg, Königstuhl, 69117 Heidelberg, Germany

Received 21 January 2010 / Accepted 1 June 2010

ABSTRACT

Context. While M dwarfs are the most abundant stars in the Milky Way, there is still large uncertainty about their basic physical properties (mass, luminosity, radius, etc.) as well as their formation environment. Precise knowledge of multiplicity characteristics and how they change in this transitional mass region, between Sun-like stars on the one side and very low mass stars and brown dwarfs on the other, provide constraints on low mass star and brown dwarf formation.

Aims. In the largest M dwarf binary survey to date, we search for companions to active, and thus preferentially young, M dwarfs in the solar neighbourhood. We study their binary/multiple properties, such as the multiplicity frequency and distributions of mass-ratio and separation, and identify short period visual binaries, for which orbital parameters and hence dynamical mass estimates can be derived in the near future.

Methods. The observations are carried out in the SDSS i' and z' band using the Lucky Imaging camera AstraLux Sur at the ESO 3.5 m New Technology Telescope. Lucky Imaging is a very efficient way of observing a large sample of stars at an angular resolution close to the diffraction limit.

Results. In the first part of the survey, we observed 124 M dwarfs of integrated spectral types M0–M6 and identified 34 new and 17 previously known companions to 44 stars. We derived relative astrometry and component photometry for these binary and multiple systems. More than half of the binaries have separations smaller than $1''$ and would have been missed in a simply seeing-limited survey. Correcting our sample for selection effects yields a multiplicity fraction of $32 \pm 6\%$ for 108 M dwarfs within 52 pc and with angular separations of $0.1''$ – $6.0''$, corresponding to projected separations of 3–180 AU at median distance 30 pc. Compared to early-type M dwarfs ($M \gtrsim 0.3 M_{\odot}$), later-type (and hence lower mass) M dwarf binaries appear to have closer separations, and more similar masses.

Key words. techniques: high angular resolution – binaries: visual – stars: low-mass – brown dwarfs

1. Introduction

M dwarfs form a link between solar-type stars and brown dwarfs, two mass regions that exhibit very different multiplicity characteristics. Because properties such as binary fraction, period distribution, and mass-ratio distribution provide important constraints on models of star formation and dynamical evolution (Goodwin et al. 2007; Burgasser et al. 2007), precise knowledge of multiplicity characteristics and how they change within this transitional mass region is important to understanding the formation of low-mass stars and brown dwarfs. Repeated astrometric observations of binary systems can also provide dynamical mass estimates, which are crucial to the empirical calibration of the mass-luminosity relation and evolutionary models. While being well known for solar-type stars, these relations are not very well constrained for lower mass stars. Theoretical models have been

shown to underpredict the masses of M dwarfs ($M \lesssim 0.5 M_{\odot}$) by 5–20%, and are particularly inconsistent for masses below $0.3 M_{\odot}$ (e.g., Hillenbrand & White 2004).

It is generally agreed upon that the binary fraction $f_{\text{bin}} = N_{\text{binaries}}/N_{\text{total}}$ decreases with decreasing stellar mass (see, e.g., review by Burgasser et al. 2007). While the binary fraction of Sun-like stars is $\approx 57\%$ (Duquennoy & Mayor 1991) over the full range of orbital separations, the fraction of multiple stars decreases to ≈ 26 – 42% for M0–M6 dwarfs (Delfosse et al. 2004; Reid & Gizis 1997; Fischer & Marcy 1992). For very low mass stars ($M < 0.1 M_{\odot}$) and brown dwarfs, the binary frequency is only 10–30% (e.g., Bouy et al. 2003; Reid et al. 2008; Joergens 2008; Goldman et al. 2008). These previous surveys of M dwarfs are limited to relatively small individual sample sizes, the largest until now being that of Delfosse et al. (2004), which consisted of 100 stars.

Whether the observed multiplicity characteristics are smooth functions of mass – implying that very low mass stars (VLMSs) and brown dwarfs (BDs) form like more massive stars – or if another process is primarily responsible for the formation of VLMSs and BDs, is debated. The multiplicity distributions of VLMSs and BDs show some important differences from those

* Based on observations made with ESO Telescopes at La Silla or Paranal Observatories under programme ID 082.C-0053.

** Tables 1 and 2 are only available in electronic form at <http://www.aanda.org>

*** Member of the International Max Planck Research School for Astronomy and Cosmic Physics at the University of Heidelberg.

of Sun-like stars. The semi-major axis distribution of VLMSs and BDs is narrow and peaks at small separations (3–10 AU, e.g., Burgasser et al. 2007), in strong contrast to the separation distribution of solar-type binaries, which is wide and peaks at around 30 AU (Duquennoy & Mayor 1991). The mass-ratio distribution also differs for VLMSs and BDs from that of Sun-like stars, showing a clear preference for equal mass binaries (e.g., Burgasser et al. 2007) as opposed to the flat distribution of the more massive stars (Duquennoy & Mayor 1991). For M dwarfs, the mass range in-between, Fischer & Marcy (1992) found a relatively flat mass-ratio distribution, while Reid & Gizis (1997) found a preference for almost equal mass systems. The differences in binary characteristics have been argued by, e.g., Thies & Kroupa (2007) to support the existence of two populations, “star-like” and “BD-like”, which are formed by different processes.

The AstraLux M dwarf survey (Hormuth et al. 2009) investigates the multiplicity characteristics of low-mass stars using high-resolution Lucky Imaging performed by the two AstraLux instruments, AstraLux Norte at the Calar Alto 2.2 m telescope (Hormuth et al. 2008) and AstraLux Sur at NTT at La Silla (Hippler et al. 2009). The full survey will include ~800 stars in the range of spectral types M0–M6 within 52 pc from the Sun, selected from the Riaz et al. (2006) catalogue of young, nearby late-type stars. The choice of observing young stars is motivated by the higher sensitivity to substellar companions, which at young ages are still warm and hence brighter and easier to detect than around older stars. A 0.072 M_{\odot} brown dwarf is 3.2 mag brighter in *I*-band at the age of 0.5 Gyr than at an age of 5 Gyr (Baraffe et al. 2003). Thus, by surveying young M dwarfs we can also detect brown dwarf companions with masses close to the stellar/substellar boundary. The large sample will allow a detailed statistical analysis of multiplicity characteristics, in the mass region between Sun-like stars and brown dwarfs where these properties change drastically. Follow-up observations of close, nearby multiple systems will also enable dynamical masses to be determined, allowing calibration of the mass-luminosity relation for stars less massive than 0.5 M_{\odot} . We present here the first southern sky sample, consisting of 124 M dwarfs.

2. Observations and data reduction

2.1. Observations

The first subsample of the 124 nearby M dwarfs presented here (see Table 1) was observed with the AstraLux Sur high resolution camera mounted at the Nasmyth B focus of the ESO 3.5 m New Technology Telescope (NTT) at La Silla on November 12–16, 2008. The targets were selected from the Riaz et al. (2006) catalogue of ≈ 1000 nearby active M dwarfs. All of our targets have spectral types M0–M6 and lie within 52 pc of the Sun. We do not have direct age estimates for more than a few individual stars (see Appendix), although the Riaz et al. (2006) sample was compiled by correlating 2MASS with ROSAT data, and the sample as a whole, based on its typically strong coronal emission and low tangential velocity ($< 40 \text{ km s}^{-1}$), is very likely young.

AstraLux Sur (Hippler et al. 2009) is a high-speed electron multiplying camera for Lucky Imaging observations at the NTT. The instrument is an almost identical copy of the common user AstraLux Norte camera at the Calar Alto 2.2 m telescope (Hormuth et al. 2008).

The Lucky Imaging principle is to minimize atmospheric seeing effects by taking many (~10000) very short

exposures (~10 ms) of the target, thereby effectively “freezing” the atmosphere in each image. Only the least distorted few percent of the frames, selected on the basis of Strehl ratio, are then combined to achieve almost diffraction-limited resolution. The Drizzle algorithm (Fruchter & Hook 2002) shifts and adds the slightly undersampled raw images by centering on the brightest pixel, thereby generating an oversampled output image with a pixel scale of $\approx 15.37 \text{ mas}$ (Hormuth et al. 2008).

On each night of observations, the M dwarf targets were observed in either the SDSS *i'* or *z'* filter. Each star was observed in full-frame mode (FoV 15.74", integration time 29.45 ms) and in some cases, if the flux was high enough, in subframe mode (FoV 7.87", integration time 15.29 ms), allowing for shorter integration times and hence less distortion by atmospheric turbulence. Twilight sky-flats were obtained whenever the weather conditions were suitable, otherwise we used dome flats. Astrometric reference stars in 47 Tuc and Trapezium (see Köhler et al. 2008) were observed several times each night, allowing us to determine the platescale and detector orientation. We assume atmospheric refraction to cause a negligible amount of field distortion (~1 mas) since separations between the binaries are small. The IRAF *geomap* procedure was used to determine the platescale of the drizzled images to be 15.373 mas/px with a mean scaling uncertainty of 0.002 mas/px, and a rotation angle of $1.71^{\circ} \pm 0.3^{\circ}$.

2.2. Photometry and astrometry of the candidate binaries/multiples

Binary separations, position angles, and magnitude differences in SDSS *i'* and *z'* filters were obtained for each binary/multiple system by fitting model PSFs from a set of reference stars (see Bouy et al. 2003). We used single stars from our observed sample with symmetric PSFs as references. The astrometric and photometric values presented are weighted averages of several measurements. The weighting is based on the residuals of the PSF fits. In our analysis, we primarily used the highest quality 10% selection of 10 000 integrations with 30 ms exposure time each, yielding a total integration time of 30 s per target and filter. In a few rare cases, we used the 1% selection to achieve a slightly higher astrometric accuracy.

Since the Lucky Imaging produces a stellar PSF with an almost diffraction-limited core and a seeing halo, high-pass filtering was implemented before fitting the model PSF when the stellar companion was much fainter than the primary star and close enough to reside within the halo. For the astrometric parameters (binary separation and position angle), we used only the *z'*-band images since they are affected by less atmospheric refraction than the *i'*-band frames. For the wide binaries (separation $\rho \gtrsim 2''$), the PSFs of the companions do not overlap and we used the IRAF aperture photometry task *phot* for the astrometry and photometry. This approach produces results with approximately the same uncertainty as the PSF fitting procedure. A combination of the two procedures was employed in a few cases for the triple systems. The dominant errors in the determined position angles arise from the uncertainty in field rotation (see Sect. 2.1) and is therefore assumed to be 0.3° for all systems. The average error in separation is 4 mas.

If the two stars are close and of similar magnitude, the Lucky Imaging drizzle combination sometimes centres on the secondary star instead of the primary, leading to the appearance of a fake third stellar component in the image. In that case, a ghost stellar image appears at the same separation from the primary but at a 180° angle from the real secondary. To recover

the flux ratio of the two “real” binary components from the fake triple, we measured the flux of the three components and used the “de-tripling” equation of Law (2006) given by

$$F_R = \frac{2I_{13}}{I_{12}I_{13} + \sqrt{I_{12}^2 I_{13}^2 - 4I_{12}I_{13}}} \quad (1)$$

where F_R is the true binary flux ratio, $I_{12} = F_1/F_2$ and $I_{13} = F_1/F_3$.

Table 1 lists the complete sample of observed stars with integrated spectral type, distance, J magnitude, and $\log[L_x/L_{\text{bol}}]$ from Riaz et al. (2006), the filter(s) in which the star was observed and corresponding epoch. Table 2 lists the astrometric and photometric properties derived for the binary/multiple systems in our sample. Component A is the primary star, which is defined as the brightest of the components in z' -band. Figure 1 shows all observed multiple systems with separations closer than $1''$, and Fig. 2 shows the wider systems with separations of between $1''$ and $5.5''$. Brightness differences achieved are typically 3.5 mag for angular separations $\sim 0.5''$ and ≥ 6 mag at $\sim 1''$ (Fig. 3).

3. Results

3.1. Stellar ages and spectral types

The observed sample is, as a whole, assumed to be young (≤ 600 Myr), based on its typically strong coronal emission and low tangential velocity (Riaz et al. 2006). As the velocity dispersion of stars steadily increases with time (e.g., Seabroke & Gilmore 2007), the low tangential velocities of smaller than 40 km s^{-1} of the stars in the Riaz et al. (2006) sample combined with activity indicators provide evidence of their youth. Holmberg et al. (2009), e.g., calibrated the age-velocity relation (AVR) for FG stars. By scaling their 3D AVR of FG stars to the tangential (2D) velocity dispersion of our sample of M dwarfs, we derive an upper age limit of ≈ 1 Gyr.

The spectral types of the individual components in the multiple systems were estimated to a precision of ± 1 subclasses following the method of Daemgen et al. (2007). We assumed that the flux ratios of the individual components obtained from the PSF fitting are linearly related to the integrated spectral types provided by Riaz et al. (2006). This relation was combined with the Kraus & Hillenbrand (2007) magnitude – spectral type relations, using linear interpolation to derive individual spectral types in 0.5 subclasses. Table 3 summarises the separate component spectral types. The spectral types were determined from observations in both filters i' and z' when available, which are in most cases consistent and otherwise noted in the Appendix. For some stars, we derived primary star spectral types that are 0.5 subclasses earlier than the integrated spectral types. The primary spectral type range for the multiple systems is thus K7.5–M5.5 (see Table 3). Only the systems where the primary star has a spectral type M0 or later are used in the statistical analysis.

The Kraus & Hillenbrand (2007) relations can be used for spectral types no later than L0. However, we estimate that five of the companions are of later spectral type. Four of these objects were only observed in z' filter (see Appendix). For these five companions, we do not determine the spectral types in any more detail than “later than L0” until we can assign more precise spectral types using future spectroscopic observations. The multiple systems containing these faint objects are excluded from the following mass ratio analysis, because of their unknown spectral types (and hence unknown masses).

3.2. Binary/multiplicity fraction

In our sample of 124 observed M dwarfs in the integrated spectral type range M0–M6, we find 51 companions belonging to 44 stars in the angular separation range $0.1''$ – $9.5''$ and z' -band magnitude difference $0 < \Delta z' < 6.9$. The observed number of single:binary:triple:quadruple stars is 80:38:5:1. However, the survey is most likely insensitive to companions fainter than $\Delta z' \geq 2$ in the angular separation range $0.1''$ – $0.5''$, and is incomplete for separations greater than $6''$ because of the small FoV. Figure 3 shows the z' -band magnitude difference achieved as a function of the component angular separation and the typical 5σ detection limit. Figure 4 depicts the number of binaries per angular separation. The distribution is strongly peaked at close separations, with more than half of the companions being within $1''$ to the primary star, suggesting that the vast majority of the observed binaries are indeed physical companions and not the product of background star contamination. While most companions were discovered in this survey (34 stars, see Table 2), some of the binaries in our sample were already known to be comoving pairs and some are confirmed here by second epoch observations (17 companions, see Table 2 and Appendix).

For the following statistical analysis (multiplicity fraction, mass ratio distribution, and separation distribution), we exclude stars/systems

- that lie farther than 52 pc from the Sun (J06061342-0337082);
- components of the binary/multiple systems with separations greater than $6''$ from the primary star (the components J06583980-2021526C, J08224744-5726530C, and the systems J21103147-2710578 and J22171899-0848122);
- binary/multiple systems for which we derive primary spectral type earlier than M0 (J01452133-3957204, J04071148-2918342, J04373746-0229282), or which are part of a wider known system containing a primary star of spectral type earlier than M0 (J04373746-0229282, J07174710-2558554);
- “single” stars that are not really single but part of a wide, known system partly outside our field of view.

This ensures that

- all the single stars in our sample are indeed single, to the best of our knowledge;
- the binary/multiple statistics is limited to stars/systems with primary spectral type M0–M6, for stars that lie within 52 pc of the Sun and have separations in the range $0.1'' \leq \rho \leq 6.0''$ (see Table 1).

The observed multiplicity frequency $f_{\text{obs}} = N_{\text{Multiple}}/N_{\text{Total}}$ is, after this selection, $35 \pm 6\%$ (Poisson errors), where N_{Multiple} is the number of binary or multiple systems (38) and N_{Total} is the number of observed systems (108). Figure 5 shows the observed multiplicity fraction for each primary spectral type. The multiple systems included in the following analysis can be found in Table 2, and the number of single:binary:triple:quadruple systems in Table 4.

To compute the actual multiplicity frequency, we need to consider two effects: (i) at small separations, we detect more equal brightness binaries than systems with large component brightness differences; and (ii) a brightness-limited sample is biased in favour of (previously unresolved) binaries or multiple systems compared to single stars.

Assuming that the flux ratio distribution is independent of the separation in the observed range (which can be transformed into a flat mass ratio distribution), we estimate the number of

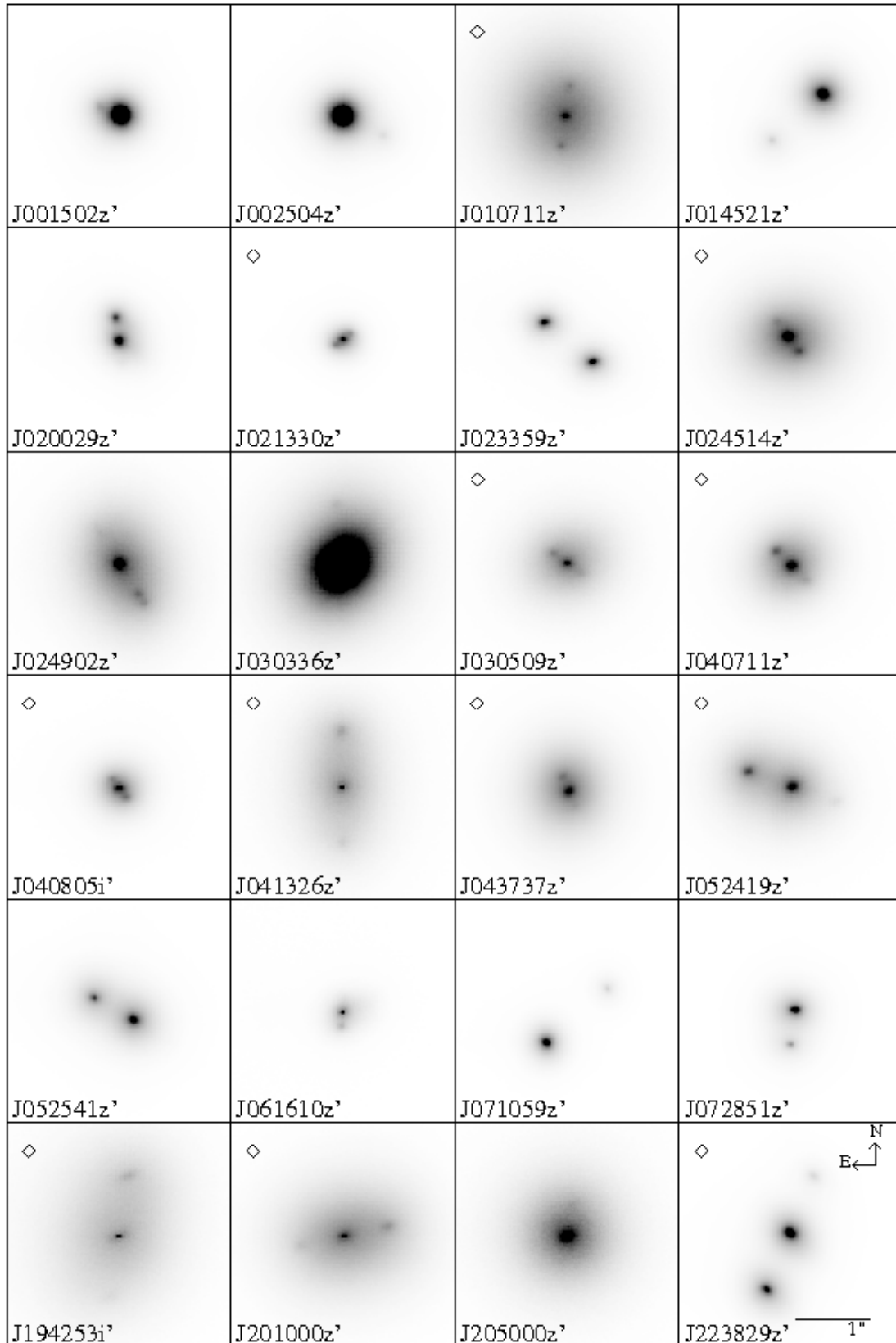


Fig. 1. AstraLux Sur images of the systems closer than $1''$. The last character in the ID refers to the filter in which the star is imaged (SDSS i' or z'). The images are shown in a logarithmic intensity scale. The scale and orientation is the same for all images and is shown in the bottom right image. The only physical triple system in the figure is J024902. What appears as a third star at 180° angle from the true secondary in some images is an effect of the Lucky Imaging drizzle combination described in Sect. 2.2. Images affected by this effect are marked with a diamond in the upper left corner.

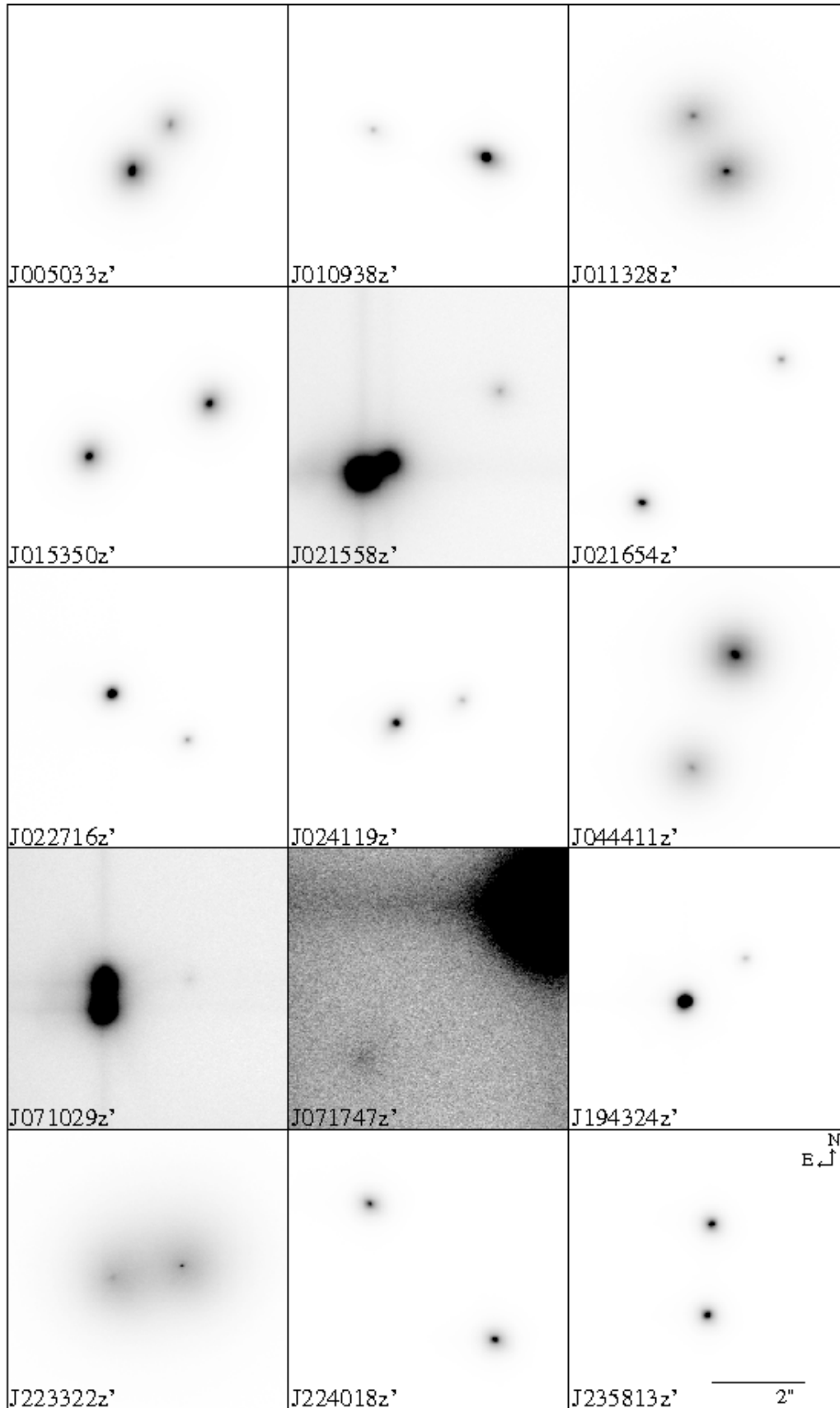


Fig. 2. AstraLux Sur images of the systems with separations between $1''$ and $5.5''$. The last character in the ID refers to the filter in which the star is imaged (SDSS i' or z'). The scale and orientation is the same for all images and is shown in the bottom right image. The images are shown in a logarithmic intensity scale, except for J021558 z' , J071029 z' , and J071747 z' , which are shown on a logarithmic square root scale.

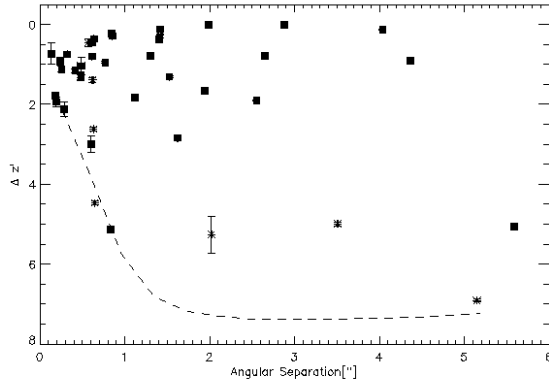


Fig. 3. Observed z' -band magnitude difference $\Delta z'$ as a function of angular separation. Squares denote binary systems and asterisks components in triple/quadruple systems. Only systems selected from the criteria in Sect. 3.2 are included. The dashed line corresponds to the typical 5σ detection limit in these observations.

multiple systems of close separations that we miss using the following method. We divide the number of binaries in Fig. 3 of observed $\Delta z'$ as a function of angular separation ρ into four different regions of interest. Assuming that our sample is complete to $\Delta z' \lesssim 5.5$ between angular separation $0.5''-3''$ and complete to $\Delta z' \lesssim 2.5$ for closer separations, the ratio of companions in the region $\rho = 0.5''-3''$, $\Delta z' = 2.5-5.5$ and $\rho = 0.5''-3''$, $\Delta z' = 0-2.5$ is the same as the ratio of companions in $\rho = 0.1''-0.5''$, $\Delta z' = 2.5-5.5$ and $\rho = 0.1''-0.5''$, $\Delta z' = 0-2.5$. This would result in the survey missing two binary companions in the close separation – high flux ratio region, hence the total multiple fraction should be increased to $37 \pm 6\%$.

We compute the multiplicity fraction for a volume-limited sample, f' , following the method and Eq. (4) of Burgasser et al. (2003)

$$f' = \frac{f'_{\text{obs}}}{f'_{\text{obs}} + \alpha(1 - f'_{\text{obs}})} \quad (2)$$

where $f'_{\text{obs}} = 0.37$ is the fraction of observed binaries after sensitivity correction. Burgasser et al. (2003) consider α values in the range 2.8, corresponding to only equal brightness systems, to 1.9, which corresponds to a flat flux ratio distribution. The distribution of z' -band brightness ratios (see Table 2) in our sample is more peaked towards unequal systems (on a linear brightness ratio scale), resulting in $\alpha = 1.73$. According to Eq. (4) of Burgasser et al. (2003), this then yields a multiplicity fraction for a volume-limited sample of $f' = 25 \pm 6\%$.

However, the Riaz et al. (2006) sample is based on a correlation of M dwarf candidates selected from the 400 million sources in the 2MASS point source catalogue (PSC, angular resolution $\sim 2''$, Cutri et al. 2003) with the 150 000 sources in the ROSAT All Sky Survey (RASS, angular resolution $\sim 30''$, Voges et al. 1999), thus the brightness limit is imposed by the X-ray luminosity of the sources. Hence, we need to correct for the excess of multiple systems as two or more stellar components emit more X-rays than the corresponding primary component would do if it were single. We can do this straightforwardly by simply examining all our a posteriori known multiple systems and determining which ones would not have been included in the sample if the primary had been single. X-ray counts and errors are available

Table 3. Individual spectral types and projected separations.

2MASS ID	Primary SpT	Secondary SpT	Separation [AU]
J00150240-7250326	M 0.5	M 3.5	11.0 ± 4.1
J00250428-3646176	M 2.5	M 5.0	16.9 ± 6.3
J00503319+2449009	M 3.5	M 4.5	15.7 ± 1.3
J01071194-1935359	M 0.5	M 2.5	12.5 ± 4.6
J01093874-0710497	M 1.0	M 4.0	97.1 ± 13.0
J01132817-3821024	M 0.0	M 1.0	52.0 ± 19.2
J01365516-0647379	M 4.0	>L0	206.7 ± 76.5
J01452133-3957204 ^a	K 7.5	M 3.5	30.2 ± 2.2
J01535076-1459503	M 3.0	M 3.0	51.8 ± 19.2
J02002975-0239579	M 3.5	M 4.5	15.5 ± 5.7
J02133021-4654505	M 4.0	M 5.0	1.8 ± 0.7
J02155892-0929121AB	M 2.5	M 5.0	16.4 ± 6.1
J02155892-0929121AC	M 2.5	M 8.0	91.2 ± 33.8
J02165488-2322133	M 3.5	M 4.5	174.8 ± 64.7
J02271603-2929263	M 3.5	M 5.0	98.9 ± 36.6
J02335984-1811525	M 3.0	M 3.5	42.7 ± 15.8
J02411909-5725185	M 2.5	M 4.0	68.7 ± 25.4
J02451431-4344102	M 4.0	M 4.5	1.8 ± 0.7
J02490228-1029220AB	M 1.5	M 3.5	16.4 ± 6.1
J02490228-1029220AC	M 1.5	M 3.5	21.2 ± 7.8
J03033668-2535329	M 0.0	M 6.0	32.5 ± 2.8
J03050976-3725058	M 1.5	M 3.0	10.9 ± 4.0
J04071148-2918342 ^a	K 7.5	M 1.0	15.1 ± 5.6
J04080543-2731349	M 3.5	M 4.5	7.8 ± 2.9
J04132663-0139211	M 4.0	M 4.0	9.3 ± 3.4
J04373746-0229282 ^{a,c}	K 7.5	M 3.0	5.1 ± 1.9
J04441107-7019247	M 1.0	M 2.5	50.4 ± 18.7
J05241914-1601153	M 4.5	M 5.0	5.1 ± 1.9
J05254166-0909123	M 3.5	M 4.0	13.6 ± 5.0
J06161032-1320422	M 3.5	M 5.0	6.0 ± 2.2
J06583980-2021526AB	M 4.0	M 4.0	45.4 ± 16.8
J06583980-2021526AC ^b	M 4.0	>L0	223.7 ± 82.8
J06583980-2021526AD	M 4.0	>L0	164.8 ± 61.0
J07102991-1637350AB	M 2.5	M 3.0	27.8 ± 10.3
J07102991-1637350AC	M 2.5	M 9.0	99.0 ± 36.6
J07105990-5632596	M 1.5	M 4.5	58.2 ± 21.6
J07174710-2558554 ^c	M 2.0	>L0	250.6 ± 92.7
J07285137-3014490	M 1.0	M 3.0	7.8 ± 0.3
J08224744-5726530AB	M 4.5	>L0	5.2 ± 1.9
J08224744-5726530AC ^b	M 4.5	M 6.0	67.4 ± 25.0
J19425324-4406278	M 3.5	M 4.5	30.1 ± 11.1
J19432464-3722108	M 3.5	M 6.0	50.3 ± 18.6
J20100002-2801410	M 2.5	M 3.5	16.0 ± 5.9
J20500010-1154092	M 3.5	M 4.5	18.5 ± 7.1
J21103147-2710578 ^b	M 4.5	M 5.5	152.0 ± 56.3
J22171899-0848122AB ^b	M 4.0	M 4.5	79.5 ± 29.4
J22171899-0848122AC ^b	M 4.0	M 8.5	77.9 ± 28.8
J22332264-0936537	M 2.5	M 3.0	37.0 ± 13.7
J22382974-6522423	M 3.5	M 3.5	12.6 ± 1.2
J22401867-4931045	M 5.5	M 5.5	40.4 ± 14.9
J23581366-1724338	M 2.0	M 2.0	55.7 ± 20.6

Notes. ^(a) The primary star spectral type is earlier than M0 (see also Appendix). The system is therefore not included in the statistical analysis. ^(b) The survey is not complete for component separations greater than $6''$ and these stars are therefore not included in the statistical analysis (see Table 2). ^(c) Our primary star is the secondary star in a known binary system in which the primary star is of spectral type F. The system is therefore not included in the statistical analysis.

from ROSAT (Voges et al. 1999) for each of the 44 multiple systems (except for one system, J20500010-1154092, which is counted as a non-detection here). Given that the components in any given system should be coeval, it is assumed that the X-ray

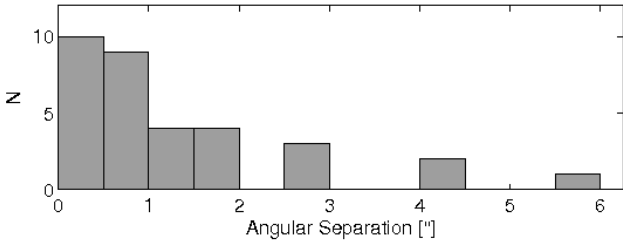


Fig. 4. Binary separation in arcsec for all observed binary systems with separation $\rho \leq 6.0''$. The triple and quadruple systems are not included. Note that more than half of the binaries are closer than $1''$, indicating that the vast majority of the binaries in the sample are physical companions and not background stars.

brightness depends only on the stellar luminosity. According to Riaz et al. (2006), L_X/L_{bol} is roughly constant as function of spectral type, hence to a reasonable approximation the X-ray count rate can be assumed to be directly proportional to the brightness fraction in z' -band in linear units. Thus, we use the known $\Delta z'$ for each system in combination with the unresolved X-ray count rate to estimate the rate for the primary component alone. If the new value results in $S/N < 3.3$, the multiple system in question is counted as having been positively selected for and is excluded for the purpose of calculating the multiple fraction for a volume-limited sample, where $S/N = 3.3$ is the relevant criterion for detection according to the tables of Voges et al. (1999). In total, 7 systems are identified as contaminants in this way. Hence, applying corrections for the X-ray flux limit as described above, it follows that the multiplicity fraction f is given by $f = (38 - 7)/(108 - 7) \times 1.053 = 32 \pm 6\%$.

While both multiplicity fractions f and f' agree within the uncertainties, in the following we assume a multiplicity fraction $f = 32 \pm 6\%$, as the brightness limit is primarily imposed by the X-ray luminosity. We note that some overabundance of short-period binaries ($P < 20$ days) might be present in the X-ray selected sample, but this cannot be quantified until future radial velocity observations have been performed. We also note that this fraction might still include a small contamination by non-physical (“optical”) binaries, as second-epoch observations for some of the systems are still pending, although we reiterate that the fraction of binaries that are merely optical must be very small (see Fig. 4).

3.3. Mass ratio distribution

The individual component photometric spectral types from Sect. 3.1 are transformed to approximate masses using the mass estimates of Kraus & Hillenbrand (2007) for young (~ 500 Myr) stars. We interpolate linearly to obtain masses for subclasses of 0.5 and calculate the mass-ratios, $q = M_2/M_1$. The binaries where the secondary star is suspected to be an L dwarf are not included in the mass-ratio distribution because of the high uncertainties in mass. We also exclude components at separations greater than $6''$ from the primary star and systems where the primary star is of spectral type earlier than M0 (see Tables 2 and 3). Since we also wish to include the triple systems in the multiplicity statistics, and all of our triple systems consist of one close pair and one wider component, we follow Reid & Gizis (1997) and calculate the triple mass-ratio as if the system consists of two separate binary systems, one close pair $q_{\text{close}} = M_B/M_A$ and one wider system with the combined mass of the close system

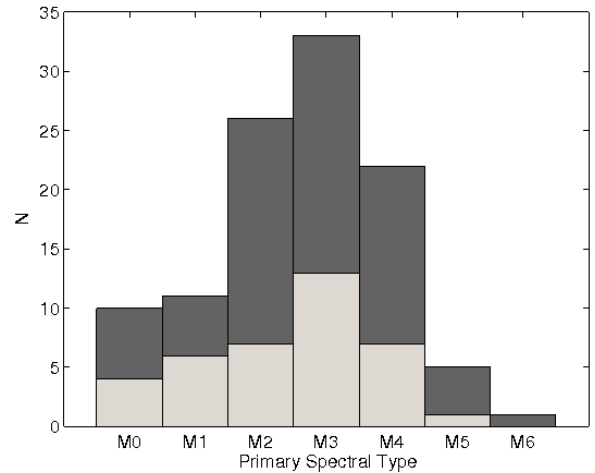


Fig. 5. Multiplicity fraction for each spectral type. The dark grey bins show all observed stars of each spectral type after selection criteria described in Sect. 3.2 have been imposed on the observed sample. The light grey bins represent the number of multiple systems in the survey.

Table 4. Number of systems used in multiplicity and mass-ratio analysis.

Fraction	Single	Binary	Triple	Quadruple
f_{Mult}	70	34	4	0
q	...	33	3	0

as the higher mass component, e.g., $q_{\text{wide}} = M_C/(M_A + M_B)$. The quadruple system J06583980-2021526 contains one close pair of spectral types M4+M4 and two more distant suspected L dwarfs, (one of which is also outside the $6''$ limit). This system is, therefore, treated as a regular binary system, ignoring the two fainter components.

The mass-ratio distribution has been seen to vary from a flat distribution among solar-type stars to peak at almost equal mass systems for VLMSs and brown dwarfs (see e.g., Allen 2007, and references therein). Figure 6 shows the mass-ratio distribution for our M0–M5.5 binaries compared to the distribution for all known VLMS and brown dwarf binaries compiled from the Very Low Mass Binaries Archive¹ (total system mass $< 0.2 M_{\odot}$). We applied small updates to the July 28, 2009 version of the archive. Almost equal mass binaries are preferred for VLMSs/brown dwarfs, but the M dwarf distribution is much flatter. While our sensitivity limit makes our survey incomplete at the low mass-ratio end of the distribution, equal mass systems should easily be seen. The lack of a peak near $q \sim 1$ is therefore a real property of the M dwarf binary systems in the separation range $0.1''$ – $6.0''$. We note that the mass-ratio distribution for VLMSs and BDs might be flatter in the case of very young systems (Burgasser et al. 2007). The samples are however very small, even if we account for more recently discovered systems, and we are therefore unable to address the age effects. No correlation between mass-ratio and component separation is seen in our sample.

When we divide our sample into early M dwarfs of primary spectral type M0–M3 ($M \gtrsim 0.3 M_{\odot}$) and late M dwarfs of spectral type M3.5–M5.5 ($M \lesssim 0.3 M_{\odot}$), we see some indication of a peak in the distribution around $q \gtrsim 0.7$ – 0.8 for the late type M dwarfs that is not present in the very flat $f(q)$ distribution of

¹ <http://www.vlmbinaries.org>

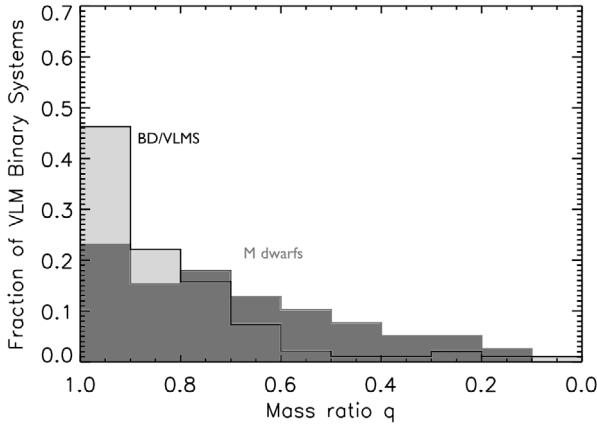


Fig. 6. Mass-ratio distribution. The dark grey distribution shows the mass-ratios of the AstraLux M dwarf binaries. The light grey distribution shows all known VLM binaries ($M < 0.2 M_{\odot}$) from the Very Low Mass Binaries Archive at <http://www.vlmbinaries.org> for comparison. Triple systems are included as two binaries as described in Sect. 3.3. Systems where one component is a suspected L dwarf, where the primary star is of spectral type earlier than M0, and companions with greater separation than $6''$ from the primary are not included.

the early type M dwarfs (see Fig. 7). Assuming that our survey is not complete for mass-ratios $q < 0.4$, a Kolmogorov-Smirnov (K-S) test shows that the probability that the “early-M” and the “late-M” mass-ratios are drawn from the same distribution is 10%. This might indicate that the shape of the mass ratio distribution is a function of mass, which approaches the $q \sim 1$ peak for the lower mass stars. However, this division into seemingly different populations should be assumed with caution. For mid-to late-M dwarfs, the mass - spectral type relation becomes very steep. Thus, a large brightness difference corresponds to only a very small change in mass for lower mass objects. Hence, a detection limit of $\Delta z' \lesssim 1.5$ magnitudes, which we assume to be valid for all stars in the sample, corresponds to a mass-ratio completeness $q \gtrsim 0.4$ for early-type M dwarfs, while the same detection limits correspond to completeness only for $q \gtrsim 0.6$ for an M3.5 primary star and $q \gtrsim 0.8$ for an M5 primary. While the missing $q \sim 1$ peak is an unbiased feature, the sensitivity to lower q values is strongly dependent on spectral type. With more observations from the full AstraLux M dwarf survey, we will be able to investigate these distributions in greater detail.

3.4. Distribution of separations

From the parallax distances, if available, and otherwise the spectroscopic distances provided by Riaz et al. (2006), we calculate the projected separation in astronomical units. The uncertainty in spectroscopic distance according to Riaz et al. (2006) is 37%. Figure 8 shows the distribution of projected separation of all binaries and triples in our M dwarf sample compared to that of all known VLMS/BD binaries from the Very Low Mass Binaries Archive.

As for the mass-ratio distribution, we divide the observed systems into two groups, containing approximately equal number of systems, to see if the separation distribution is the same for “early M” and “late M” type binaries divided at $M \approx 0.3 M_{\odot}$. Figure 9 shows the respective mean semi-major axis distributions, where the projected separation has been multiplied

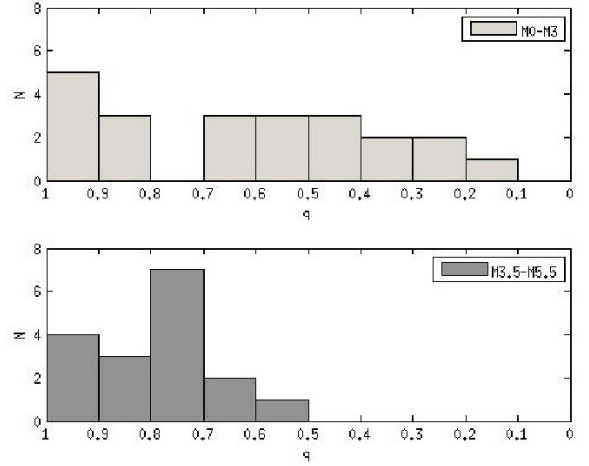


Fig. 7. Mass-ratio distribution divided into early-M type primaries (M0–M3) and late-M type (M3.5–M5.5). Triple systems are included as described in Sect. 3.3. Systems where one component is a suspected L dwarf and components at separations greater than $6''$ are not included.

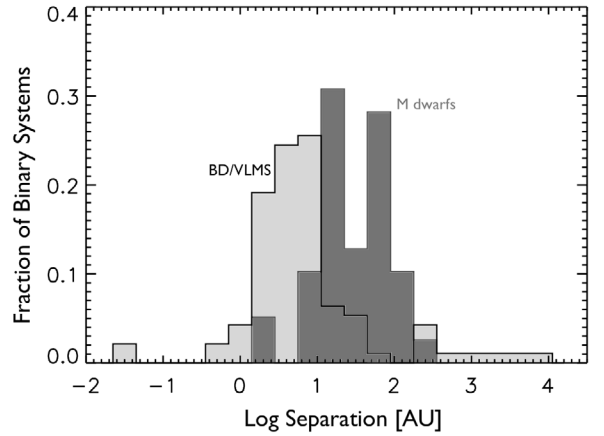


Fig. 8. Projected separation distributions. The darker grey shows the M dwarf binaries/triples in our sample and the light grey shows VLMS/BD binaries from the Very Low Mass Binaries Archive.

with 1.26 to account for random orbital elements (Fischer & Marcy 1992). We performed a K-S test, which yielded a 9% probability that the distributions are alike. We note that the distributions may peak at close systems in the “late M” subsample, however more data is necessary to determine whether this is a real property or not.

4. Discussion

M dwarfs comprise a transitional region within which the multiplicity properties change from being similar to those of solar-type stars to the very different characteristics of very low mass stars and brown dwarfs. Smaller surveys of different mass ranges have provided some insight into the transitional behaviour.

We observed 124 nearby M dwarfs from the Riaz et al. (2006) catalogue. Forty-four of our targets were observed to have potential binary/multiple companions within $0.1''$ – $9.5''$ of

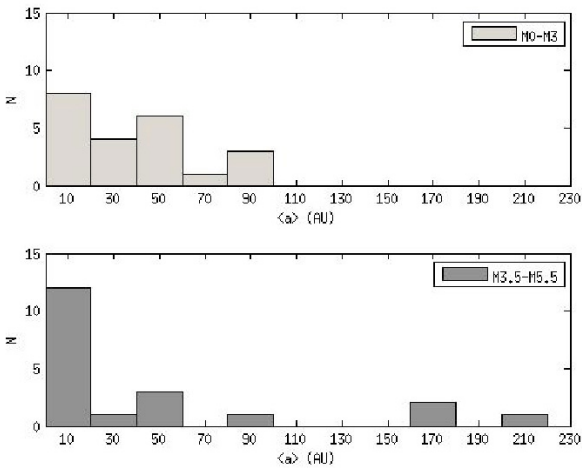


Fig. 9. Distribution of mean semi-major axis for “early M” and “late M” primary spectral types. The binaries are divided into two groups: “early type M”, consisting of the binaries with a primary spectral type M0–M3, and “late type M” for primary spectral types M3.5–M5.5. All separations are measured from the primary stars.

the primary star. Most of these companions were previously unknown.

We have estimated the multiplicity fraction for M0–M6 young ($\lesssim 600$ Myr) dwarfs with angular separations $0.1''$ – $6''$, corresponding to projected separation 3–180 AU at median distance 30 pc, in this largest sample to date to be $32 \pm 6\%$. While differences in the binary fraction have been found in various nearby star-forming regions (Leinert et al. 1993; Ghez et al. 1993; Brandner & Köhler 1998; Köhler et al. 2006), observations of the 90 Myr old α Persei and the 600 Myr old Praesepe clusters suggest that the companion star fraction does not significantly decline over an age range from 90 Myr to 5 Gyr (Patience et al. 2002). We therefore did not expect there to be a strong evolution in binary properties from ages ~ 100 Myr to a few Gyr. Our derived f_{Mult} is consistent with previous surveys in the same mass and separation range for field dwarfs (e.g., the multiplicity fraction of the Fischer & Marcy (1992) sample for M0–M4 systems with linear separation $2.6 < a < 300$ AU is $f_{\text{bin}} = 28 \pm 9\%$, according to Close et al. 2003) and young M dwarfs (23% for < 300 Myr M0–M5 binaries with separations 1.6–300 AU, Daemgen et al. 2007). This is a higher f_{Mult} than found in high resolution imaging surveys of later type M field dwarfs (e.g., Law et al. (2008) 13.6% for M4.5–M6; Close et al. (2003) 15% for M8–L0.5; Siegler et al. (2005) 9% for M6–M7.5).

Previous large investigations inferred different behaviours for the mass ratio distribution of M dwarfs. For instance, Fischer & Marcy (1992) found that the mass ratio distribution for M0–M6 dwarfs is relatively flat for the full orbital separation range, while Reid & Gizis (1997) found a strong peak for $q \gtrsim 0.8$. However, Delfosse et al. (2004) showed in their large survey that the distribution of mass-ratio is relatively flat for orbital periods $P > 50$ days, while shorter period binaries tend to have equal masses.

When considering only systems in the survey of Reid & Gizis (1997) with M dwarf primaries (M0.5–M5.5) and mean semi-major axis $3.7 < a < 227$ AU, the same region probed in this survey, we find that the distribution is flat (although the sample is very small with only 16 companions). We therefore expect our distribution to be flat as well, in accordance with those

of other surveys. We have found that the mass-ratio distribution of all binaries in the primary spectral type range M0–M5.5 is flatter than the distribution for VLMSs and BDs and does not exhibit the prominent peak at $q \sim 1$ detected for the VLMS/BD sample. This is consistent with the results of Reid & Gizis (1997) over the same range of linear separations, and a real feature for M dwarfs in the observed separation range not affected by observational incompleteness. To investigate the transitional properties, we divided our sample into two groups of “early M” and “late M” primary stars and found that the “early M” distribution is relatively flat, while there might be a preference for more similar mass binaries in the “late M” group. Future analysis of the full AstraLux M dwarf survey will allow us to investigate this possible trend in more detail.

Thies & Kroupa (2007) argued that the differences in binary characteristics of stars and brown dwarfs point to different but related formation processes for these two populations. In their survey of M4.5–M6 binaries, Law et al. (2008) found a bimodal separation distribution where the later type M dwarfs peak at close separations as seen for brown dwarfs, but some of the earlier systems have projected separations greater than 10 AU. This is indicative of a change in the separation distributions at spectral type \sim M5, consistent with the Thies & Kroupa (2007) predictions of two separate but overlapping populations. For later type M dwarfs, Siegler et al. (2005) find no binaries with separations $a > 10$ AU in their high-resolution imaging survey of M6–M7.5 field dwarfs covering separations 3–300 AU, and Close et al. (2003) find no binaries wider than 16 AU for the M8–L0.5 dwarfs in the same separation range. We divide our separation distribution into “early M” and “late M” groups at $M \sim 0.3 M_{\odot}$. Even though our sample contains somewhat more massive stars than that of Law et al. (2008), the distribution of “early M” multiples is flatter than the “late M” distribution in which more than half of the companions reside within 20 AU of the primary star. While our results are still subject to relatively large statistical uncertainties, we note that they may indicate that a bimodal distribution also exist for larger separations and higher masses than the sample of Law et al. (2008). This will be investigated further in the larger sample of the complete survey.

These results show that Lucky Imaging with AstraLux Sur is very efficient at detecting binary stars with small angular separations. Several of our newly discovered companions presented here have been found to be close to the diffraction limit ($\sim 0.1''$). Future follow-up observations with AstraLux Sur will allow us to determine orbital motions and hence dynamical masses for the closest nearby systems.

Acknowledgements. We thank the anonymous referee for helpful comments and suggestions leading to an improved paper. This publication has made use of the Very-Low-Mass Binaries Archive housed at <http://www.vlmbinaries.org> and maintained by Nick Siegler, Chris Gelino, and Adam Burgasser. This research has made use of the SIMBAD database, operated at CDS, Strasbourg, France.

Appendix A: Notes on individual binaries and multiple systems

Table 5 summarises our measured angular separations and position angles, and published results for previously known components.

J00503319+2449009 This star, also known as GJ 3060A or NLTT 2805, is a flare star (Norton et al. 2007) with a known stellar companion, NLTT 2804. The Catalog of Components of Double & Multiple Stars (CCDM, Dommanget & Nys 2002)

Table 5. Separations and position angles for previously known multiple systems.

2MASS ID	ρ ["]	θ [°]	Epoch	Ref.
J00503319+2449009	1.0	315	1960	1
	2.080	316.0	1991.25	2
	1.648	317.12	2002.64	3
	1.305	318.9	2008.86	4
J01093874-0710497	2.680	77.0	1991.25	2
	2.554	74.5	2008.87	4
J02165488-2322133	4.3	315	1998.67	5
	4.369	314.1	2008.87	4
J04132663-0139211	0.79	217.11	1998.9	6
	0.771	358.8/178.8	2008.88	4
J04373746-0229282	0.225	195	2003.05	7
	0.093	189.5	2004.95	7
	0.221	20.5	2008.88	4
J04441107-7019247	2.3	174	1990	8
	2.654	157.5	2008.88	4
J05254166-0909123	0.537	69.40	2005.78	9
	0.616	58.8	2008.86	4
J07285137-3014490	0.175	143.71	2002.83	9
	0.485	169.9	2008.86	4
J08224744-5726530	8.6	23	1999.99	5
	8.429	26.1	2008.88	4
J21103147-2710578	9.4	313	1998.59	5
	9.501	313.2	2008.87	4
J22171899-0848122AB	7.8	213	1998.79	5
	7.95	213.2	2008.87	4
J22171899-0848122BC	0.978	305.8	2001.60	10
	0.97	316.7	2008.87	4
J22332264-0936537	1.66	272.25	1997.6	6
	1.571	279.73	2005.44	9
	1.421	98.6/278.6	2008.87	4
J22382974-6522423	0.770	16	1991.25	2
	0.842	155.8	2008.87	4
J22401867-4931045	4.2	40	1999.72	5
	4.039	41.0	2008.87	4
J23581366-1724338	1.904	355.3	2005.54	9
	1.989	355.7	2008.87	4

References. (1) Dommanget & Nys (2002); (2) Perryman & ESA (1997); (3) Strigachev & Lampens (2004); (4) This work; (5) Cutri et al. (2003); (6) McCarthy et al. (2001); (7) Kasper et al. (2007); (8) Mason et al. (2001); (9) Daemgen et al. (2007); (10) Beuzit et al. (2004).

provides the astrometric measurements $\rho = 1.0''$ and $\theta = 315^\circ$ for epoch 1960. *Hipparcos* observations provide positions of the two components of $\rho = 2.080''$ and $\theta = 316^\circ$ (epoch 1991.25, Perryman & ESA 1997). Strigachev & Lampens (2004) present photometric and astrometric observations of visual double stars and for this binary estimate the angular

separation to be $\rho = 1.648''$ and the position angle $\theta = 317.12^\circ$ (epoch 2002.64). Our measured separation is $\rho = 1.305''$ and position angle $\theta = 318.9^\circ$, indicating orbital motion.

J01093874-0710497 This is a high proper motion star with $\mu_{RA} = -235.5$ mas/yr and $\mu_{Dec} = -351.6$ mas/yr. Also known as HIP 5443, it is a *Hipparcos* double star (Perryman & ESA 1997) with separation $\rho = 2.7''$ and position angle $\theta = 77^\circ$ (epoch 1991.25). We measure the separation $\rho = 2.554''$ and position angle $\theta = 74.5^\circ$, hence both components form a common proper motion pair. The small change in separation and position angle in the more than 15 years that have passed between the *Hipparcos* and our measurements can be attributed to orbital motion.

J01365516-0647379 The primary star is a high proper motion star for which Shkolnik et al. (2009) estimated an age between 25 and 300 Myr. Because of its faint magnitude, the secondary star could not be seen at the time of observation but only after additional analysis. The star therefore ended up partly outside the field of view in the i' -band observation and we present only z' -band data in this paper.

J02165488-2322133 In 2MASS PSC (Cutri et al. 2003), we find the star J02165465-2322103 at separation $\rho = 4.3''$ and position angle $\theta = 315^\circ$ from our primary (epoch 1998.67), which corresponds well to our measured separation $\rho = 4.369''$ and position angle $\theta = 314.1^\circ$.

J02335984-1811525 In this double system, the B component is brighter than the A component in i' -band. Since the i' and z' band observations were performed on different nights, the unusual $i' - z'$ colour might indicate that the star is variable or possibly of T Tauri-type. We tentatively assign spectral types $M3 \pm 1 + M3.5 \pm 1$ to the stars, but further investigation of this couple is necessary to determine their characteristics.

J02490228-1029220 The B and C components of this triple star are close, $\rho_{BC} = 0.145''$ corresponding to 4.93 AU.

J03033668-2535329 The primary star is a high proper motion star also known as NLTT 9775. We measure a separation $\rho = 0.834''$ between the two companions. A possible candidate for the secondary star is the high proper motion star LTT 1453, which has J2000 coordinates $RA = 03h03m36.6s$, $Dec = -25^\circ35'33''$, at an angular separation of $1.42''$ from our primary star. Frankowski et al. (2007) studied the binary content of the *Hipparcos* catalogue, listing the primary star as a candidate proper motion binary.

J04080543-2731349 The images in both i' - and z' -band of this binary are affected by “fake tripling”. The real B component and the fake triple are equally bright in z' -band but unequal in i' . This means that, although unlikely, the true position angle might be systematically incorrect by 180° .

J04132663-0139211 This binary system was discovered by McCarthy et al. (2001), with a separation $\rho = 0.79''$ and position angle $\theta = 217.11^\circ$ (epoch 1998.9). We measure $\rho = 0.771''$ and $\theta = 358.8^\circ$, indicating significant orbital motion between observations. In our observations, the B component is brighter than the A component in i' -band. Since the i' and z' band observations were performed on different nights, the unusual $i' - z'$ colour may indicate that the star is variable or possibly of T Tauri-type. If our secondary star is the primary star of McCarthy et al. (2001), the position angle is instead $\rho = 178.8^\circ$. We tentatively assign the stars spectral types $M4 \pm 1 + M4 \pm 1$, but further investigation of this double system is needed to determine its character.

J04373746-0229282 The primary star is also known as GJ 3305, a member of the young β Pictoris moving group (Zuckerman et al. 2001), which has an estimated age of 12 Myr (Shkolnik et al. 2009). The faint close companion that we see was discovered by Kasper et al. (2007) in their L-band NACO

imaging of young, nearby stars in search of substellar companions. [Kasper et al. \(2007\)](#) present NACO K-band data from the ESO/ST-ECF Science Archive with which they determine the separation $\rho = 0.225''$ and position angle $\theta = 195^\circ$ (epoch 2003.05), and their obtained L-band data for which $\rho = 0.093''$ and position angle $\theta = 189.5^\circ$ (epoch 2004.95), and the proper motion combined points to a bound companion in a highly eccentric orbit. Our observations are affected by the stellar companion ghost image at 180° discussed in Sect. 2.2, which may cause uncertainty in the true position angle. However, the assumed position at $\rho = 0.221''$ and $\theta = 20.5^\circ$ is consistent with physical companionship, and with the non-detection of the secondary companion by [Daemgen et al. \(2007\)](#) (epoch 2005.74) indicates that the orbit has a high inclination, i.e., is seen close to edge-on.

[Feigelson et al. \(2006\)](#) agree with [Zuckerman et al. \(2001\)](#) and conclude from the proper motion and stellar activity that GJ 3305 is part of a wide binary system ($\rho = 66''$, or ~ 2000 AU at 30 pc) with the F0 star 51 Eri. Since the primary star is then of earlier spectral type than M0, the system is not included in our statistical analysis.

J04441107-7019247 This is a previously known visual binary, also known as HD 270712. [Mason et al. \(2001\)](#) provides the astrometric measurements $\rho = 2.3''$ and $\theta = 174^\circ$ for epoch 1990. We measure $\rho = 2.654''$ and $\theta = 157.5^\circ$, indicating orbital motion.

J05254166-0909123 This high proper motion binary (NLTT 15049) was discovered by [Daemgen et al. \(2007\)](#), at a separation of $\rho = 0.537''$ and position angle $\theta = 69.40^\circ$ (epoch 2005.78). We assign spectral types M3.5+M4 to the couple, consistent with the spectral types of [Daemgen et al. \(2007\)](#). We find a separation $\rho = 0.616''$ and position angle $\theta = 58.8^\circ$, indicating significant orbital motion. [Shkolnik et al. \(2009\)](#) estimates the age of the stars to be between 35 and 300 Myr.

J06583980-2021526 This possibly quadruple system consists of one close M4+M4 pair and two more distant suspected L dwarfs. The two faintest components (C and D) are separated from the brightest star by $5.15''$ and $6.99''$, respectively, and had not been discovered at the time of observation. They therefore ended up outside the FoV in i' -band. The separation between components A and B is $\rho_{AB} = 1.420''$, and the two faint stars C and D are separated by $\rho_{CD} = 2.093''$ with position angle $\theta_{CD} = 107.3^\circ$. The separation between the primary star and the C component is greater than our completeness limit, and the component is therefore not included in the statistical analysis.

J07102991-1637350 The tertiary companion is too faint in i' for accurate photometry and astrometry. We therefore present only z' -band data in this paper.

J07105990-5632596 We obtain different spectral types for the secondary star in i' and z' ($\text{SpT}_{i'} \approx \text{M}5.5$, $\text{SpT}_{z'} \approx \text{M}4$). Since we did not observe the stars in both filters on the same night, the brightness of either companion might have changed from one observation to the next if the stars are variable. We tentatively assign the secondary spectral type $\text{M}4.5 \pm 1$.

J07174710-2558554 Our primary star is also known as CD-25 4322B, the secondary star in a wide double system with CD-25 4322. Our wide but faint secondary component is not, however, found in any catalogue. The star CD-25 4322 is an F-star (F0/F3V, [Dommanget & Nys 2002](#); [Perryman & ESA 1997](#)) and not within our field of view (CCDM separation $\rho = 12.4''$, epoch 1897, [Dommanget & Nys 2002](#)). Because of the faintness of our secondary companion, it was not detected at the time of observation and not observed in i' . Since our primary star

is the secondary star in a system with an F-star primary, it is not included in the statistical analysis.

J07285137-3014490 This is a known binary system also known as GJ 2060 ([Zuckerman et al. 2004](#)), which was concluded by [Allen & Reid \(2008\)](#) to probably be part of a quadruple system with another close, equal mass M dwarf binary at a separation of $\rho = 67.2''$. GJ 2060 is a likely member of the ~ 50 Myr old AB Dor association ([Zuckerman et al. 2004](#)). We obtain spectral types M1+M3, while [Daemgen et al. \(2007\)](#) find spectral types M0.5+M1.5. The primary star is a known variable star (V372 Pup). [Daemgen et al. \(2007\)](#) determine the binary separation and position angle to be $\rho = 0.175''$ and $\theta = 143.71^\circ$ (epoch 2002.83), while we find $\rho = 0.485''$ and $\theta = 169.9^\circ$, indicating significant orbital motion.

J08224744-5726530 The primary star of this triple system is also known as LHS 2005, a high proper motion star. Our separation and position angle for the tertiary component, which is also known as LHS 2004, is $\rho = 8.429''$ and $\theta = 26.1^\circ$. This is consistent with data from the 2MASS PSC ([Cutri et al. 2003](#)) for the star J08224787-5726451 with a separation $8.6''$ and position angle $\theta = 23^\circ$ (epoch 1999.99) and is indicative of orbital motion. LHS 2004 and LHS 2005 form a known common proper motion pair. The close secondary was not previously known. The wide companion was noticed at the time of observation and fitted into the field of view by placing the primary star in the corner of the detector for the z' -band observations. The wide companion is outside the field of view in i' -band. Since the C component separation from the primary is greater than $6''$, it is not included in the statistical analysis.

J19425324-4406278 The secondary star is previously unknown. Only i' -band images could be used in our analysis since the secondary star was too faint in z' . The position angle, separation, and individual spectral types are therefore obtained from the i' -band observation.

J21103147-2710578 The companion is J21103096-2710513 at a 2MASS PSC distance of $9.4''$ and position angle $\theta = 313^\circ$ (epoch 1998.59, [Cutri et al. 2003](#)). We find a separation $\rho = 9.50''$, which is greater than our limits for completeness. The system is therefore not included in the statistical analysis.

J22171899-0848122 This is a known visual binary system where the primary star (also known as V* FG Aqr or GJ 852A) and the secondary star (J22171870-0848186, or GJ 852B) are both flare stars ([Gershberg et al. 1999](#)). The tertiary companion, close to our secondary star GJ 852B at $\rho_{BC} = 0.97''$ and $\theta_{BC} = 316.7^\circ$, was discovered by [Beuzit et al. \(2004\)](#) at $\rho = 0.978''$ and $\theta = 305.8^\circ$ (epoch 2001.60), hence the system shows orbital motion. The C component is in our observations too faint to be resolved in i' band. Photometric measurements in i' for the B component therefore include the very faint flux from the close C component. The 2MASS PSC ([Cutri et al. 2003](#)) infer a proximity of $7.8''$ and position angle of $\theta = 213^\circ$ (epoch 1998.79), relating the positions of GJ 852 A and GJ 852 B. Our measured separation between these stars is $\rho = 7.95''$ and position angle $\theta = 213.2^\circ$.

J22332264-0936537 Also known as GJ 4282, this flare star was discovered to be a binary by [McCarthy et al. \(2001\)](#), who derived a separation of $\rho = 1.66''$ and position angle $\theta = 272.25^\circ$ for epoch 1997.6. [Daemgen et al. \(2007\)](#) observed a separation of $\rho = 1.571''$ and $\theta = 279.73^\circ$ for epoch 2005.44. We find $\rho = 1.421''$ and $\theta = 98.6^\circ$, a separation that agrees with previous observations but at a position angle that is clearly inconsistent with the previous measurements by [Daemgen et al. \(2007\)](#) and [McCarthy et al. \(2001\)](#). With an estimated orbital period of approximately 380 years, we need to assume that our primary

star (the eastern component) is actually the secondary star of [Daemgen et al. \(2007\)](#) and [McCarthy et al. \(2001\)](#), and our revised position angle is in that case $\theta = 278.6^\circ$, indicating orbital motion. Since in our observations the eastern star is slightly brighter than the western component, one or both of the stars might be variable, causing the discrepancy in position angle between our observations and the observations by [McCarthy et al. \(2001\)](#) and [Daemgen et al. \(2007\)](#). We assign the stars spectral types M 2.5 and M 3, respectively, in agreement with [Daemgen et al. \(2007\)](#) (M 3+M 3) and [Shkolnik et al. \(2009\)](#) (eastern component M 2.5, western component M 2.6). [Shkolnik et al. \(2009\)](#) estimate the age of the system to be 20–150 Myr.

J22382974-6522423 This flare star, which is also known as GJ 865, was identified by [Montes et al. \(2001\)](#) as a possible member of the ~600 Myr Hyades supercluster. The star GJ 865 is part of a known triple system. We observed the two close components, separated by $\rho = 0.842''$, which is in agreement with the separation $\rho = 0.770''$ and position angle $\theta = 16^\circ$ found by [Perryman & ESA \(1997\)](#) for epoch 1991.25. The third companion is outside our field of view, with a separation from our primary star of $\rho = 30.4''$ (epoch 1974, [Dommanget & Nys 2002](#)). While we could not find the spectral type of this companion in literature, the V magnitudes of the three companions differ only slightly ($V_A = 12.0$, $V_B = 12.1$, $V_C = 12.3$, [Dommanget & Nys 2002](#), where the close components are B and C) and we assume that the third component is also an M star. We therefore include this system in the binary statistics as an M dwarf binary/multiple system.

J22401867-4931045 This couple of high proper motion stars ([Lépine 2005](#)) are also known as LSR J22403-4931W (our primary star) and LSR J22403-4931E located at RA = 22h 40m 18.96s, Dec = $-49^\circ 31' 01.4''$ (J2000). [Cutri et al. \(2003\)](#) found $\rho = 4.2''$ and $\theta = 40^\circ$ for epoch 1999.72. We measure $\rho = 4.039''$ and $\theta = 41.0^\circ$.

J23581366-1724338 The binary character of this high proper motion star, also known as NLTT 58589, was discovered by [Daemgen et al. \(2007\)](#), who derived the same individual spectral types M 2+M 2, as we do. We find $\rho = 1.989''$, in good agreement with the [Daemgen et al. \(2007\)](#) separation $\rho = 1.904''$ for epoch 2005.54, although our measured position angle $\theta = 355.7^\circ$ disagrees with the [Daemgen et al. \(2007\)](#) result of $\theta = 265.30^\circ$ by 90° . Reanalysis of the Gemini data by [Daemgen et al.](#) yields a position angle of 355.3° , which is in good agreement with the AstraLux Sur measurement and indicates some orbital motion. [Shkolnik et al. \(2009\)](#) determine individual spectral types M 1.9 (north)+M 1.9 (south) and an age of 20–150 Myr for the system.

J23534173-6556543: We also observed this star, which is the secondary star in a widely separated G 0 V+M 1 V system, and its primary. The primary is HIP 117815 and the secondary is CPD-66 3810B. Our separation of $\rho = 12.3''$ at $\theta = 112.2^\circ$ is in good agreement with [Eggenberger et al. \(2007\)](#) ($\rho = 12.14''$, $\theta = 112.37^\circ$, epoch 2005.70) for this bound system. This system was only observed in z' -band and is not included in any statistical analysis in this paper because the primary star is a G star.

References

- Allen, P. R. 2007, *ApJ*, 668, 492
 Allen, P. R., & Reid, I. N. 2008, *AJ*, 135, 2024
 Baraffe, I., Chabrier, G., Barman, T. S., Allard, F., & Hauschildt, P. H. 2003, *A&A*, 402, 701
 Beuzit, J., Ségransan, D., Forveille, T., et al. 2004, *A&A*, 425, 997
 Bouy, H., Brandner, W., Martín, E. L., et al. 2003, *AJ*, 126, 1526
 Brandner, W., & Köhler, R. 1998, *ApJ*, 499, L79
 Burgasser, A. J., Kirkpatrick, J. D., Reid, I. N., et al. 2003, *ApJ*, 586, 512
 Burgasser, A. J., Reid, I. N., Sieglar, N., et al. 2007, in *Protostars and Planets V*, ed. B. Reipurth, D. Jewitt, & K. Keil, 427
 Close, L. M., Sieglar, N., Freed, M., & Biller, B. 2003, *ApJ*, 587, 407
 Cutri, R. M., Skrutskie, M. F., van Dyk, S., et al. 2003, 2MASS All Sky Catalog of point sources., ed. R. M. Cutri, M. F. Skrutskie, S. van Dyk, C. A. Beichman, J. M. Carpenter, T. Chester, L. Cambresy, T. Evans, J. Fowler, J. Gizis, E. Howard, J. Huchra, T. Jarrett, E. L. Kopan, J. D. Kirkpatrick, R. M. Light, K. A. Marsh, H. McCallon, S. Schneider, R. Stiening, M. Sykes, M. Weinberg, W. A. Wheaton, S. Wheelock, & N. Zacarias
 Daemgen, S., Sieglar, N., Reid, I. N., & Close, L. M. 2007, *ApJ*, 654, 558
 Delfosse, X., Beuzit, J.-L., Marchal, L., et al. 2004, in *Spectroscopically and Spatially Resolving the Components of the Close Binary Stars*, ed. R. W. Hilditch, H. Hensberge, & K. Pavlovski, ASP Conf. Ser., 318, 166
 Dommanget, J., & Nys, O. 2000, *VizieR Online Data Catalog*, 1260, 0
 Dommanget, J., & Nys, O. 2002, *VizieR Online Data Catalog*, 1274, 0
 Duquenois, A., & Mayor, M. 1991, *A&A*, 248, 485
 Eggenberger, A., Udry, S., Chauvin, G., et al. 2007, *A&A*, 474, 273
 Feigelson, E. D., Lawson, W. A., Stark, M., Townsley, L., & Garmire, G. P. 2006, *AJ*, 131, 1730
 Fischer, D. A., & Marcy, G. W. 1992, *ApJ*, 396, 178
 Frankowski, A., Jancart, S., & Jorissen, A. 2007, *A&A*, 464, 377
 Fruchter, A. S., & Hook, R. N. 2002, *PASP*, 114, 144
 Gershberg, R. E., Katsova, M. M., Lovkaya, M. N., Terebizh, A. V., & Shakhovskaya, N. I. 1999, *A&AS*, 139, 555
 Ghez, A. M., Neugebauer, G., & Matthews, K. 1993, *AJ*, 106, 2005
 Goldman, B., Bouy, H., Zapatero Osorio, M. R., et al. 2008, *A&A*, 490, 763
 Goodwin, S. P., Kroupa, P., Goodman, A., & Burkert, A. 2007, *Protostars and Planets V*, 133
 Hillenbrand, L. A., & White, R. J. 2004, *ApJ*, 604, 741
 Hippler, S., Bergfors, C., Brandner, W., et al. 2009, *The Messenger*, 137, 14
 Holberg, J. B., Oswalt, T. D., & Sion, E. M. 2002, *ApJ*, 571, 512
 Holmberg, J., Nordström, B., & Andersen, J. 2009, *A&A*, 501, 941
 Hormuth, F., Hippler, S., Brandner, W., Wagner, K., & Henning, T. 2008, in *Society of Photo-Optical Instrumentation Engineers (SPIE) Conf. Ser.*, 7014
 Hormuth, F., Brandner, W., Janson, M., Hippler, S., & Henning, T. 2009, in *American Institute of Physics Conference Series*, ed. E. Stempels, 1094, 935
 Joergens, V. 2008, *A&A*, 492, 545
 Kasper, M., Apai, D., Janson, M., & Brandner, W. 2007, *A&A*, 472, 321
 Köhler, R., Petr-Gotzens, M. G., McCaughrean, M. J., et al. 2006, *A&A*, 458, 461
 Köhler, R., Ratzka, T., Herbst, T. M., & Kasper, M. 2008, *A&A*, 482, 929
 Kraus, A. L., & Hillenbrand, L. A. 2007, *AJ*, 134, 2340
 Law, N. 2006, Ph.D. Thesis Institute of Astronomy & Selwyn College, Cambridge University
 Law, N. M., Hodgkin, S. T., & Mackay, C. D. 2008, *MNRAS*, 384, 150
 Leinert, C., Zinnecker, H., Weitzel, N., et al. 1993, *A&A*, 278, 129
 Lépine, S. 2005, *AJ*, 130, 1247
 Mason, B. D., Wycoff, G. L., Hartkopf, W. I., Douglass, G. G., & Worley, C. E. 2001, *AJ*, 122, 3466
 McCarthy, C., Zuckerman, B., & Becklin, E. E. 2001, *AJ*, 121, 3259
 Montes, D., López-Santiago, J., Gálvez, M. C., et al. 2001, *MNRAS*, 328, 45
 Norton, A. J., Wheatley, P. J., West, R. G., et al. 2007, *A&A*, 467, 785
 Patience, J., Ghez, A. M., Reid, I. N., & Matthews, K. 2002, *AJ*, 123, 1570
 Perryman, M. A. C., & ESA 1997, *The HIPPARCOS and TYCHO catalogues. Astrometric and photometric star catalogues derived from the ESA HIPPARCOS Space Astrometry Mission*, ESA SP, 1200
 Reid, I. N., & Gizis, J. E. 1997, *AJ*, 113, 2246
 Reid, I. N., Cruz, K. L., Allen, P., et al. 2004, *AJ*, 128, 463
 Reid, I. N., Cruz, K. L., Burgasser, A. J., & Liu, M. C. 2008, *AJ*, 135, 580
 Riaz, B., Gizis, J. E., & Harvin, J. 2006, *AJ*, 132, 866
 Seabroke, G. M., & Gilmore, G. 2007, *MNRAS*, 380, 1348
 Shkolnik, E., Liu, M. C., & Reid, I. N. 2009, *ApJ*, 699, 649
 Sieglar, N., Close, L. M., Cruz, K. L., Martín, E. L., & Reid, I. N. 2005, *ApJ*, 621, 1023
 Strigachev, A., & Lampens, P. 2004, *A&A*, 422, 1023
 Thies, I., & Kroupa, P. 2007, *ApJ*, 671, 767
 Torres, C. A. O., Quast, G. R., da Silva, L., et al. 2006, *A&A*, 460, 695
 van Altena, W. F., Lee, J. T., & Hoffleit, E. D. 1995, *The general catalogue of trigonometric [stellar] parallaxes*, ed. W. F. van Altena, J. T. Lee, & E. D. Hoffleit
 Voges, W., Aschenbach, B., Boller, T., et al. 1999, *A&A*, 349, 389
 Zuckerman, B., Song, I., Bessell, M. S., & Webb, R. A. 2001, *ApJ*, 562, L87
 Zuckerman, B., Song, I., & Bessell, M. S. 2004, *ApJ*, 613, L65

Table 1. Properties of all stars observed 11–16 November 2008.

2MASS ID	Other name	SpT ^a	D [pc] ^a	J mag ^a	$\log [L_x/L_{\text{bol}}]$ ^a	Filter	Epoch ^b
J00150240-7250326 ^c		M 1.0	38	8.62	-3.01	i', z'	2008.86
J00155808-1636578		M 4.0	9	8.74	-3.08	z'	2008.87
J00171443-7032021		M 0.5	48	9.00	-3.23	i', z'	2008.87
J00213729-4605331	GJ 3029	M 3.0	20 ^d	8.33	-2.56	z'	2008.87
J00250428-3646176 ^c		M 2.5	28	8.65	-3.30	i', z'	2008.86
J00275035-3233238 ^g		M 3.5	28	8.97	-2.75	i', z'	2008.86
J00281434-3227556		M 5.0	12	10.12	-2.85	z'	2008.86
J00503319+2449009 ^c	GJ 3060A	M 3.5	12 ^d	7.92	-3.06	i', z'	2008.86
J01025097+1856543		M 4.0	13	9.51	-3.24	z'	2008.86
J01071194-1935359 ^c		M 1.0	30	8.15	-3.13	i', z'	2008.87
J01093874-0710497 ^c	HIP 5443	M 1.5	38 ^d	7.96	-3.70	i', z'	2008.87
J01112343-0525381		M 3.5	35	9.47	-2.86	z'	2008.87
J01132817-3821024 ^c		M 0.5	37	8.49	-3.19	i', z'	2008.88
J01225093-2439505		M 3.5	45	10.08	-3.18	z'	2008.88
J01244246-1540454 ^h	NLTT 4703	M 1.5	27	8.11	-4.01	z'	2008.88
J01365516-0647379 ^c	NLTT 5400	M 4.0	37	9.70	-2.89	z'	2008.86
J01434512-0602400		M 3.5	26	8.77	-3.00	i', z'	2008.86
J01452133-3957204 ^c	NLTT 5871	M 0.0	32 ^d	8.43	-3.81	i', z'	2008.86
J01511997+1324525		M 1.5	31	8.56	-3.21	z'	2008.86
J01535076-1459503 ^c		M 3.0	18	7.94	-3.12	i', z'	2008.86
J02001277-0840516		M 2.5	30	8.77	-3.11	i', z'	2008.86
J02002975-0239579 ^c		M 3.5	48	10.07	-2.95	i', z'	2008.87
J02014384-1017295	NLTT 6782	M 4.0	17	10.03	-3.34	z'	2008.87
J02070198-4406444		M 5.5	21	11.36	-2.26	z'	2008.87
J02070786-1810077		M 4.0	22	10.70	-2.73	z'	2008.87
J02133021-4654505 ^c		M 4.0	13	9.43	-2.99	i', z'	2008.87
J02155892-0929121 ^c		M 2.5	26	8.43	-3.11	i', z'	2008.87
J02164119-3059181 ⁱ	GJ 3148 A	M 3.5	14 ^d	7.99	-3.42	z'	2008.87
J02165488-2322133 ^c		M 3.5	40	9.79	-2.50	i', z'	2008.87
J02183655+1218579		M 2.0	34	8.80	-3.40	z'	2008.87
J02224418-6022476		M 4.0	10	8.99	-2.58	z'	2008.87
J02271603-2929263 ^c		M 3.5	51	10.34	-3.27	i', z'	2008.87
J02303485-1543248	NLTT 8185	M 2.5	39	9.29	-3.31	z'	2008.87
J02335984-1811525 ^c		M 3.0	50	10.09	-2.77	i', z'	2008.87
J02365171-5203036		M 2.0	28	8.42	-3.01	z'	2008.87
J02411510-0432177	NLTT 8687	M 4.0	11	9.20	-3.64	z'	2008.87
J02411909-5725185 ^c		M 3.0	45	9.85	-3.15	i', z'	2008.87
J02414730-5259306		M 2.5	27	8.48	-2.65	z'	2008.87
J02451431-4344102 ^c		M 4.0	7	8.06	-3.26	i', z'	2008.88
J02485260-3404246		M 4.0	12	9.31	-2.90	z'	2008.88
J02490228-1029220 ^c		M 2.0	34	8.82	-3.21	i', z'	2008.88
J02492136-4416063		M 3.0	45	9.88	-3.30	z'	2008.88
J02543316-5108313		M 1.5	34	8.67	-3.33	z'	2008.88
J03033668-2535329 ^c	NLTT 9775	M 0.0	39 ^d	8.00	-3.65	i', z'	2008.88
J03050976-3725058 ^c		M 2.0	45	9.54	-3.50	i', z'	2008.88
J03100305-2341308	NLTT 10115	M 3.5	35	9.41	-3.29	z'	2008.88
J03152341-2821404		M 3.5	49	10.25	-2.41	z'	2008.86
J03214689-0640242	GJ 3218	M 2.0	16 ^e	7.86	-4.74	z'	2008.86
J03244056-3904227		M 4.0	40	9.87	-2.27	z'	2008.86
J03271433+2723087	NLTT 10933	M 0.5	27 ^d	8.64	-3.44	z'	2008.86
J03432333-0819412		M 2.5	49	9.86	-3.62	z'	2008.88
J03472333-0158195	NLTT 11853	M 2.5	16 ^d	7.80	-3.14	z'	2008.88
J04071148-2918342 ^c		M 0.0	51	9.06	-3.16	i', z'	2008.88
J04080543-2731349 ^c		M 3.5	43	9.89	-3.14	i', z'	2008.88
J04093930-2648489		M 1.5	49	9.51	-3.11	z'	2008.88
J04132663-0139211 ^c		M 4.0	12	9.38	-2.97	i', z'	2008.88
J04141730-0906544		M 3.5	37	9.63	-2.70	z'	2008.88
J04175717-3827038		M 3.5	36	9.45	-2.91	z'	2008.88
J04213904-7233562		M 2.5	50	9.87	-2.97	z'	2008.88
J04240094-5512223		M 2.5	48	9.80	-3.26	z'	2008.88
J04241156-2356365		M 2.5	24	8.32	-3.70	i', z'	2008.88
J04353618-2527347	NLTT 13598	M 3.5	20	8.24	-3.24	i', z'	2008.88
J04365738-1613065		M 3.5	30	9.12	-2.63	i', z'	2008.88
J04373746-0229282 ^c	GJ 3305	M 0.0	23	7.30	-2.71	i', z'	2008.88
J04380252-0556132	NLTT 13666	M 4.5	12	9.73	-3.05	z'	2008.88
J04441107-7019247 ^c	HD 270712	M 1.5	19	7.46	-3.62	i', z'	2008.88
J04522441-1649219	NLTT 14116	M 3.0	18	7.74	-3.17	i', z'	2008.88
J05082729-2101444		M 5.0	11	9.72	-3.19	i', z'	2008.88
J05241914-1601153 ^c		M 4.5	8	8.67	-3.14	i', z'	2008.88
J05254166-0909123 ^c	NLTT 15049	M 3.5	22	8.45	-3.18	i', z'	2008.86
J05332802-4257205		M 4.5	6	8.00	-3.13	i', z'	2008.88
J06045215-3433360		M 5.0	4	7.74	-2.95	i', z'	2008.88
J06061342-0337082 ^j		M 2.5	57	10.15	-3.03	i', z'	2008.88

Table 1. continued.

2MASS ID	Other name	SpT ^a	D [pc] ^a	J mag ^a	$\log [L_x/L_{\text{bol}}]$ ^a	Filter	Epoch ^b
J06161032-1320422 ^c		M 4.0	31	11.35	-2.32	i', z'	2008.87
J06224133-2737531		M 3.5	35	9.43	-3.21	z'	2008.87
J06253604-4815598		M 2.5	34	9.10	-3.74	z'	2008.87
J06255610-6003273		M 3.5	19	8.09	-2.90	z'	2008.87
J06525392-0524413		M 2.5	30	8.71	-3.17	z'	2008.87
J06583980-2021526 ^c		M 4.0	32	9.40	-3.23	i', z'	2008.87
J07020886-0626206		M 2.0	52	9.80	-2.67	z'	2008.87
J07065772-5353463		M 0.0	41	8.54	-3.17	z'	2008.87
J07102991-1637350 ^c		M 2.5	49	9.75	-3.02	i', z'	2008.87
J07105990-5632596 ^c		M 1.5	52	9.61	-2.43	i', z'	2008.87
J07120447-3048526		M 2.5	47	9.71	-3.44	z'	2008.87
J07174710-2558554 ^c		M 2.0	47	9.53	-3.19	z'	2008.88
J07285137-3014490 ^c	GJ 2060	M 1.5	16 ^d	6.62	-3.04	i', z'	2008.86
J08224744-5726530 ^c	LHS 2005	M 4.5	8	8.63	-3.14	i', z'	2008.88
J19425324-4406278 ^c		M 3.5	36	9.43	-3.12	i', z'	2008.87 ^m
J19432464-3722108 ^c		M 3.5	31	9.20	-3.31	i', z'	2008.87
J19513587-3510375		M 4.0	8	8.58	-3.23	z'	2008.87
J20100002-2801410 ^c		M 3.0	26	8.65	-3.16	i', z'	2008.87
J20194981-5816431		M 6.0	12	10.66	-2.28	i', z'	2008.87
J20500010-1154092 ^c		M 3.5	38	9.68	-3.58	i', z'	2008.87
J21010793-4158536		M 0.0	52	8.98	-3.46	z'	2008.87
J21073678-1304581		M 3.0	27	8.73	-3.16	z'	2008.87
J21103147-2710578 ^c		M 4.5	16	10.30	-3.00	i', z'	2008.87
J21235271-3908176		M 3.5	32	9.33	-3.36	z'	2008.87
J21505366-0553186		M 1.0	51	9.38	-3.04	z'	2008.87
J21574119-5100221 ^k	GJ 841 A	M 2.5	16 ^d	6.75	-3.17	i', z'	2008.87
J22114208-2044181		M 3.5	39	9.65	-3.18	i', z'	2008.87
J22171899-0848122 ^c	GJ 852 A	M 4.0	10	9.02	-2.75	i', z'	2008.87
J22174316-1546452		M 4.0	22	10.79	-2.83	z'	2008.87
J22184009-5326405		M 2.5	37	9.24	-3.25	i', z'	2008.87
J22230696-1736250	GJ 4274	M 4.0	7 ^f	8.24	-3.26	z'	2008.87
J22332264-0936537 ^c	GJ 4282	M 2.5	26	8.53	-2.96	i', z'	2008.87
J22382974-6522423 ^c	GJ 865	M 3.5	15 ^d	7.27	-3.37	i', z'	2008.87
J22401867-4931045 ^c		M 5.5	10	9.84	-2.90	i', z'	2008.87
J23115362-4508004 ^l	HD 218860B	M 3.0	44	9.72	-2.54	i', z'	2008.88
J23131671-4933154		M 4.0	15	9.76	-2.68	z'	2008.87
J23261069-7323498		M 0.0	46	8.84	-3.09	z'	2008.87
J23285763-6802338		M 2.5	38	9.26	-3.07	i', z'	2008.87
J23314492-0244395	GJ 1285	M 4.5	11	9.51	-2.76	i', z'	2008.87
J23320018-3917368		M 3.0	29	8.90	-2.83	i', z'	2008.88
J23323085-1215513		M 0.0	25	7.45	-3.15	z'	2008.87
J23324655-1645081 ⁿ	GI 897	M 2.5	12	6.71	-3.30	z'	2008.87
J23341101-1531012 ^o		M 0.0	47	8.91	-3.30	z'	2008.87
J23452225-7126505		M 3.5	48	10.19	-2.88	z'	2008.87
J23474694-6517249		M 1.5	42	9.10	-3.42	z'	2008.87
J23483610-2739385	GJ 4362	M 2.5	27	8.58	-3.23	z'	2008.87
J23532520-7056410		M 3.5	24	8.68	-3.53	z'	2008.87
J23555512-1321238	NLTT 58441	M 2.5	39	9.26	-3.46	z'	2008.87
J23571934-1258406 ^p	GJ 4379 B	M 3.0	32	9.13	-2.88	z'	2008.87
J23572056-1258487 ^p	GJ 4378 A	M 4.0	23	8.64	-3.03	z'	2008.87
J23581366-1724338 ^c	NLTT 58589	M 2.0	28	8.31	-3.14	i', z'	2008.87

Notes. ^(a) Integrated spectral types, J magnitude, and $\log[L_x/L_{\text{bol}}]$ from Riaz et al. (2006). Distance is spectroscopic distance from Riaz et al. (2006) if not otherwise indicated. The uncertainty in the spectroscopic distances is 37%. ^(b) Epoch of z' -band observations, for which the astrometric properties of the multiple systems are derived. ^(c) Binary/multiple system observed with AstraLux, see Tables 2 and 3 for properties. ^(d) Parallax distance from *Hipparcos* (Perryman & ESA 1997). ^(e) Parallax distance from Reid et al. (2004). ^(f) Parallax distance from van Altena et al. (1995). ^(g) This is one component of a wide ($\rho = 19.9''$, epoch 2001) visual double-star system (Mason et al. 2001). The system is therefore not included in the statistical analysis. ^(h) This is the secondary component of a wide multiple system with the G-type primary star NLTT 4704. The system is therefore not included in the statistical analysis. ⁽ⁱ⁾ This is the primary component of a *Hipparcos* visual double system, with the secondary component outside our field of view at $\rho = 105.0''$ (epoch 1991.25, Dommanget & Nys 2000). The system is not included in the statistical analysis. ^(j) The target J06061342-0337082 has spectroscopic distance 57 pc and is therefore not included in the multiplicity analysis. ^(k) The star is part of a wide binary system with the white dwarf GJ 841 B (Holberg et al. 2002) and is therefore not included in the statistical analysis. ^(l) The star is part of a wide binary system with the primary G8V star HD 218860A (Torres et al. 2006) and is therefore not included in the statistical analysis. ^(m) Epoch refers to the i' -band observation, from which astrometric properties were derived. ⁽ⁿ⁾ The star is part of a multiple system in which the K6V star (Torres et al. 2006) GI 898 is the primary (Dommanget & Nys 2000). The star is therefore not included in the statistical analysis. ^(o) The star is part of a wide binary system (Mason et al. 2001) and is therefore not included in the statistical analysis. ^(p) The star is part of a common proper motion system (Mason et al. 2001) and is therefore not included in the statistical analysis.

Table 2. Photometric and astrometric properties of the observed binary/multiple M dwarfs.

Primary ID (2MASS)	$\Delta z'$	$\Delta i'$	ρ [$''$]	θ [$^\circ$]	New ^a (y/n)	f_{Mult}^b	q^c
J00150240-7250326	2.13 ± 0.18	1.31 ± 0.14	0.290 ± 0.009	69.1 ± 0.3	y	y	y
J00250428-3646176	2.99 ± 0.21	2.59 ± 0.23	0.605 ± 0.012	242.4 ± 0.3	y	y	y
J00503319+2449009	0.79 ± 0.01	0.94 ± 0.02	1.305 ± 0.002	318.9 ± 0.3	n	y	y
J01071194-1935359	1.16 ± 0.05	0.65 ± 0.03	0.417 ± 0.001	170.0 ± 0.3	y	y	y
J01093874-0710497	1.90 ± 0.01	2.02 ± 0.01	2.554 ± 0.001	74.5 ± 0.3	n	y	y
J01132817-3821024	0.37 ± 0.01	0.22 ± 0.01	1.405 ± 0.003	29.0 ± 0.3	y	y	y
J01365516-0647379	5.07 ± 0.01	...	5.587 ± 0.004	179.9 ± 0.3	y	y	n
J01452133-3957204 ^d	2.00 ± 0.10	2.39 ± 0.16	0.943 ± 0.009	130.9 ± 0.3	y	n	n
J01535076-1459503	0.01 ± 0.01	0.13 ± 0.01	2.876 ± 0.001	291.9 ± 0.3	y	y	y
J02002975-0239579	0.75 ± 0.06	0.89 ± 0.05	0.323 ± 0.001	5.9 ± 0.3	y	y	y
J02133021-4654505	0.73 ± 0.27	1.45 ± 0.08	0.135 ± 0.001	124.9 ± 0.3	y	y	y
J02155892-0929121AB	2.62 ± 0.05	2.80 ± 0.05	0.631 ± 0.001	292.2 ± 0.3	y	y	y
J02155892-0929121AC	4.99 ± 0.05	5.52 ± 0.10	3.509 ± 0.002	299.3 ± 0.3	y	y	y
J02165488-2322133	0.91 ± 0.01	0.92 ± 0.01	4.369 ± 0.001	314.1 ± 0.3	n	y	y
J02271603-2929263	1.67 ± 0.02	1.77 ± 0.01	1.939 ± 0.001	236.8 ± 0.3	y	y	y
J02335984-1811525	0.29 ± 0.01	-1.02 ± 0.05	0.854 ± 0.001	48.9 ± 0.3	y	y	y
J02411909-5725185	1.31 ± 0.02	1.47 ± 0.02	1.526 ± 0.001	287.1 ± 0.3	y	y	y
J02451431-4344102	1.12 ± 0.07	0.87 ± 0.03	0.257 ± 0.001	214.6 ± 0.3	y	y	y
J02490228-1029220AB	1.33 ± 0.06	1.42 ± 0.12	0.481 ± 0.006	209.5 ± 0.3	y	y	y
J02490228-1029220AC	1.39 ± 0.06	1.49 ± 0.11	0.622 ± 0.012	210.7 ± 0.3	y	y	y
J03033668-2535329	5.14 ± 0.06	3.69 ± 0.16	0.834 ± 0.005	7.6 ± 0.3	n	y	y
J03050976-3725058	0.93 ± 0.10	0.94 ± 0.07	0.242 ± 0.004	53.7 ± 0.3	y	y	y
J04071148-2918342 ^d	0.70 ± 0.05	0.48 ± 0.20	0.295 ± 0.001	44.4 ± 0.3	y	n	n
J04080543-2731349	1.78 ± 0.06	1.00 ± 0.10	0.181 ± 0.005	218.1 ± 0.3	y	y	y
J04132663-0139211	0.95 ± 0.02	-0.45 ± 0.03	0.771 ± 0.001	358.8 ± 0.3	n	y	y
J04373746-0229282 ^{d,f}	1.39 ± 0.16	2.57 ± 0.05	0.221 ± 0.002	20.5 ± 0.3	n	n	n
J04441107-7019247	0.79 ± 0.01	1.09 ± 0.01	2.654 ± 0.001	157.5 ± 0.3	n	y	y
J05241914-1601153	0.36 ± 0.03	0.43 ± 0.01	0.639 ± 0.001	69.1 ± 0.3	y	y	y
J05254166-0909123	0.45 ± 0.07	0.53 ± 0.09	0.616 ± 0.004	58.8 ± 0.3	n	y	y
J06161032-1320422	1.94 ± 0.12	1.40 ± 0.23	0.194 ± 0.008	170.6 ± 0.3	y	y	y
J06583980-2021526AB	0.25 ± 0.01	0.33 ± 0.01	1.420 ± 0.001	199.0 ± 0.3	y	y	y
J06583980-2021526AC ^e	5.89 ± 0.02	...	6.992 ± 0.002	263.3 ± 0.3	y	n	n
J06583980-2021526AD	6.91 ± 0.03	...	5.149 ± 0.001	253.9 ± 0.3	y	y	n
J07102991-1637350AB	0.46 ± 0.09	0.64 ± 0.05	0.568 ± 0.001	354.9 ± 0.3	y	y	y
J07102991-1637350AC	5.26 ± 0.46	...	2.021 ± 0.008	287.6 ± 0.3	y	y	y
J07105990-5632596	1.83 ± 0.07	4.17 ± 0.07	1.120 ± 0.006	309.8 ± 0.3	y	y	y
J07174710-2558554 ^f	6.35 ± 0.04	...	5.332 ± 0.002	126.8 ± 0.3	y	n	n
J07285137-3014490	1.29 ± 0.11	1.50 ± 0.18	0.485 ± 0.002	169.9 ± 0.3	n	y	y
J08224744-5726530AB	4.47 ± 0.04	5.32 ± 0.05	0.648 ± 0.002	128.7 ± 0.3	y	y	n
J08224744-5726530AC ^e	1.83 ± 0.04	...	8.429 ± 0.001	26.1 ± 0.3	n	n	n
J19425324-4406278	...	1.39 ± 0.11	0.836 ± 0.002	349.8 ± 0.3	y	y	y
J19432464-3722108	2.84 ± 0.08	2.89 ± 0.07	1.623 ± 0.004	303.7 ± 0.3	y	y	y
J20100002-2801410	0.80 ± 0.04	0.75 ± 0.03	0.615 ± 0.001	280.4 ± 0.3	y	y	y
J20500010-1154092	1.04 ± 0.22	1.17 ± 0.20	0.486 ± 0.046	348.3 ± 0.3	y	y	y
J21103147-2710578 ^e	1.07 ± 0.01	1.20 ± 0.01	9.501 ± 0.003	313.2 ± 0.3	n ^g	n	n
J22171899-0848122AB ^e	0.62 ± 0.03	0.74 ± 0.01	7.954 ± 0.001	213.2 ± 0.3	n	n	n
J22171899-0848122AC ^e	3.77 ± 0.03	...	7.794 ± 0.003	220.1 ± 0.3	n	n	n
J22332264-0936537	0.12 ± 0.01	0.65 ± 0.05	1.421 ± 0.028	98.6 ± 0.3	n	y	y
J22382974-6522423	0.23 ± 0.01	0.20 ± 0.02	0.842 ± 0.001	155.8 ± 0.3	n	y	y
J22401867-4931045	0.14 ± 0.01	0.16 ± 0.01	4.039 ± 0.001	41.0 ± 0.3	n	y	y
J23581366-1724338	0.01 ± 0.01	0.03 ± 0.01	1.989 ± 0.001	355.7 ± 0.3	n	y	y

Notes. ^(a) Companion discovered in this survey (y) or previously known (n). ^(b) Included in multiplicity fraction analysis (y/n). ^(c) Included in mass-ratio analysis (y/n). ^(d) The primary star spectral type is earlier than M0 (see Table 3). The system is therefore not included in the statistical analysis. ^(e) The survey is not complete for component separations greater than 6'' and these stars are therefore not included in the statistical analysis. ^(f) Our primary star is the secondary star in a known binary system in which the primary star is of spectral type F. The system is therefore not included in the statistical analysis. ^(g) The companion is the star 2MASS J21103096-2710513. Although the position of the secondary star is previously known, we could find no references to the couple as a common proper motion pair.